INTERNATIONAL JOURNAL FOR NUMERICAL METHODS IN FLUIDS
Int. J. Numer. Meth. Fluids 2002; **40**:1527–1538 (DOI: 10.1002/fld.409)

Iterative substructuring methods for incompressible non-isothermal flows and its application to indoor air flow simulation

T. Knopp[1,*], G. Lube[1,†], R. Gritzki[2] and M. Rösler[2]

[1] *Mathematics Department, University of Göttingen, NAM, D-37073 Göttingen, Germany*
[2] *Faculty of Mechanical Engineering, Dresden University of Technology, D-01062 Dresden, Germany*

SUMMARY

The parallel solution of the incompressible Navier–Stokes equations coupled with the energy equation is considered. For turbulent flows, the k/ε model together with a modified wall-function concept is used. The iterative process requires the fast solution of advection–diffusion reaction and Oseen-type problems. These linearized problems are discretized using stabilized finite element methods. We apply a coarse–granular iterative substructuring method which couples the subdomain problems via Robin-type interface conditions. Then we apply the approach to the simulation of indoor air flow problems. Copyright © 2002 John Wiley & Sons, Ltd.

KEY WORDS: Navier–Stokes equations; buoyancy driven air flow; turbulence

1. MATHEMATICAL MODEL

Let $\Omega \subset \mathbf{R}^d$, $d = 2, 3$ be a bounded polyhedral domain. As the basic mathematical model we consider the (non-dimensional) incompressible, non-isothermal Reynolds averaged Navier–Stokes equations (RANS) with the eddy-viscosity hypothesis. Buoyancy effects are taken into account using the Boussinesq approximation. We seek a velocity field $\mathbf{u}$, a pressure p, and a temperature θ as solutions of the coupled non-linear system

$$\begin{aligned} \partial_t \mathbf{u} - \boldsymbol{\nabla} \cdot (2\nu_e S(\mathbf{u})) + (\mathbf{u} \cdot \boldsymbol{\nabla})\mathbf{u} + \boldsymbol{\nabla} p &= -\beta\theta\mathbf{g} \\ \boldsymbol{\nabla} \cdot \mathbf{u} &= 0 \\ \partial_t \theta + (\mathbf{u} \cdot \boldsymbol{\nabla})\theta - \boldsymbol{\nabla} \cdot (a_e \boldsymbol{\nabla}\theta) &= \dot{q}^V / c_p \end{aligned} \tag{1}$$

with $S(\mathbf{u}) := \frac{1}{2}(\boldsymbol{\nabla}\mathbf{u} + \boldsymbol{\nabla}\mathbf{u}^T)$, isobaric volume expansion coefficient β, gravitational acceleration $\mathbf{g}$, volumetric heat source $\dot{q}^V$ and specific heat capacity (at constant pressure) c_p. Furthermore,

* Correspondence to: G. Lube, Department of Mathematics, University of Gottingen, NAM, D-37083 Göttingen, Germany.
† E-mail: lube@math.uni-goettingen.de

Received 1 November 2001
Revised 12 June 2002

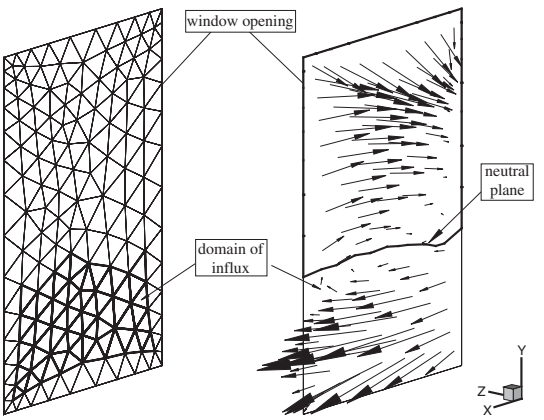

Figure 1. Inflow and outflow regions at an opened window.

we introduce the effective viscosities $\nu_e = \nu + \nu_t$ and $a_e = a + a_t$ with kinematic viscosity ν, turbulent viscosity ν_t, thermal diffusivity a and turbulent thermal diffusivity a_t.

For *turbulent* flows we apply the k/ε model [1, 2]. Turbulent effects are modelled as additional turbulent viscosity $\nu_t = c_\mu k^2/\varepsilon$ with $c_\mu = 0.09$ and thermal diffusivity $a_t = \nu_t/Pr_t$, using the turbulent kinetic energy k and turbulent dissipation ε. The latter quantities are solutions of additional diffusion–advection reaction (ADR) equations

$$\begin{aligned} \partial_t k + (\mathbf{u}\cdot\nabla)k - \nabla\cdot(\nu_k \nabla k) &= P_k + G - \varepsilon \\ \partial_t \varepsilon + (\mathbf{u}\cdot\nabla)\varepsilon - \nabla\cdot(\nu_\varepsilon \nabla \varepsilon) + C_2 \varepsilon^2 k^{-1} &= C_1 \varepsilon k^{-1}(P_k + G) \end{aligned} \tag{2}$$

with constants $C_1 = 1.44$, $C_2 = 1.92$, $C_t = 0.8$, $Pr_t = 0.9$, $Pr_k = 1.0$, $Pr_\varepsilon = 1.3$, effective viscosities $\nu_k = \nu + \nu_t/Pr_k$, $\nu_\varepsilon = \nu + \nu_t/Pr_\varepsilon$, production and buoyancy terms

$$P_k := 2\nu_t |S(\mathbf{u})|^2, \quad G := C_t \beta a_t \mathbf{g}\cdot\nabla\theta$$

The laminar case is recovered if we set $k \equiv 0$ and skip Equations (2).

Depending on the sign of $\mathbf{u}\cdot\mathbf{n}$, the boundary is divided into wall zones $\Gamma_0(\mathbf{u})$, inlet zones $\Gamma_-(\mathbf{u})$ and outlet zones $\Gamma_+(\mathbf{u})$. In Figure 1 we present the example of an opened window. Using $\tau = 2\nu_e S(\mathbf{u})$, we set

$$(\tau - pI)\mathbf{n} = \tau_n \mathbf{n} \quad \text{on } \Gamma_N \subset \Gamma_- \cup \Gamma_+, \quad \mathbf{u} = \mathbf{u}_b \quad \text{on } \Gamma_D \subset \Gamma_- \cup \Gamma_+ \tag{3}$$

with $\Gamma_D \cap \Gamma_N = \emptyset$ and $\bar{\Gamma}_D \cup \bar{\Gamma}_N = \bar{\Gamma}_- \cup \bar{\Gamma}_+$. On Γ_0, we prescribe either a no-slip condition or the tangential stresses and the normal velocity

$$\text{(i) } \mathbf{u} = \mathbf{0} \quad \text{or} \quad \text{(ii) } (I - \mathbf{n}\otimes\mathbf{n}) 2\nu_e S(\mathbf{u})\mathbf{n} = \boldsymbol{\tau}_t, \quad \mathbf{u}\cdot\mathbf{n} = 0 \quad \text{on } \Gamma_0 \tag{4}$$

In this paper, we consider only the case $\Gamma_D = \emptyset$ and replace condition (4)(i) with (ii), cf. Section 2. For θ we require

$$\gamma(\theta - \theta_{in}) + (1-\gamma) a_e \nabla\theta\cdot\mathbf{n} = 0 \quad \text{on } \bar{\Gamma}_- \cup \bar{\Gamma}_+, \quad a_e \nabla\theta\cdot\mathbf{n} = \frac{\dot{q}_0}{c_p} \quad \text{on } \Gamma_0 \tag{5}$$

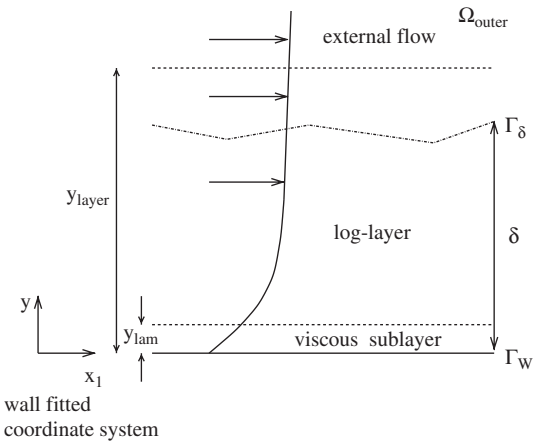

Figure 2. Domain decomposition in the boundary layer region.

Here we denote by $\gamma=\gamma(\Gamma_-)$ the characteristic function of $\bar{\Gamma}_-$. Note that the so-called neutral zone $\overline{\Gamma_-(\mathbf{u})}\cap\overline{\Gamma_+(\mathbf{u})}$, cf. Figure 1, is not *a priori* known, see also Example 2 in Section 5.

2. DOMAIN DECOMPOSITION FOR NEAR WALL LAYERS

In order to avoid an expensive spatial resolution of boundary layer regions and to circumvent adjusting c_μ there we apply, for *turbulent* flows, the concept of wall functions in the vicinity Ω_δ of a wall Γ_0 containing at least the so-called viscous sublayer, cf. Figure 2. We apply an overlapping domain decomposition method (DDM).

(I) *Outer solution*: First we solve the RANS (1) in Ω with boundary conditions (4), (5) where the r.h.s. $\boldsymbol{\tau}_t$ and $\dot{q}_0$ on walls $\Gamma_0=\Gamma_W$ have to be determined, cf. step II.
Then we solve the k/ε-equations (2) in $\Omega\backslash\Omega_\delta$. Dirichlet data are prescribed on $\Gamma_-(\mathbf{u})$ and on the artificial boundary $\Gamma_\delta=\partial\Omega_\delta\cap\Omega$. A do-nothing condition is specified on $\Gamma_+(\mathbf{u})$. More precisely, we set

Zone	$\Gamma_-(\mathbf{u})$	Γ_δ	$\Gamma_+(\mathbf{u})$
k	$k=1.5(T_u u)^2$	$k=c_\mu^{-1/2}U_*^2$	$\nu_k\nabla k\cdot\mathbf{n}=0$
ε	$\varepsilon=c_\mu^{3/4}k^{3/2}/L$	$\varepsilon=U_*^3/(\kappa y)$	$\nu_\varepsilon\nabla\varepsilon\cdot\mathbf{n}=0$

with appropriate constant κ and problem dependent data L and T_u. (The effective viscosity ν_e in (1) is modified in the wall layer region Ω_δ according to step II. Alternatively, one can solve (2) in Ω using homogeneous Neumann conditions on Γ_0 for k and ε, cf. [1].)

(II) *Compute boundary layer solution in Ω_δ and match solutions*: We introduce a wall-fitted co-ordinate system (x, y) with y being the distance from the wall Γ_W. Following [3], we simplify the RANS (1) under standard assumptions in Prandtl's boundary layer theory and using modified viscosities in Ω_δ

$$\nu_e = \nu \max\left(1; \frac{Re}{Re_{\min}}\right), \quad a_e = \frac{\nu}{Pr} \max\left(1; \frac{Pr}{Pr_t^{BL}} \frac{Re}{Re_{\min}}\right)$$

with local Reynolds number $Re(x, y) = \|\mathbf{u}(x, y)\| y/\nu$, $Pr = 0.71$, $Pr_t^{BL} = 1.16$, and an appropriate constant $Re_{\min}$. Then we seek the near wall layer approximation, for each $x \in \Gamma_W$, as the solution (u_x^{BL}, θ^{BL}) of the boundary value problems

$$\begin{aligned} -\frac{d}{dy}\left(\nu_e \frac{du_x^{BL}}{dy}\right) &= \beta \theta^{BL} g_x \\ -\frac{d}{dy}\left(a_e \frac{d\theta^{BL}}{dy}\right) &= 0 \\ u_x^{BL}|_{y=0} = 0, \quad \theta^{BL}|_{y=0} &= \theta_w \end{aligned} \tag{6}$$

g_x denoting the tangential component of $\mathbf{g}$, with matching conditions

$$u_x^{BL}|_{y=y_\delta} = u_x(y_\delta), \quad \theta^{BL}|_{y=y_\delta} = \theta(y_\delta) \tag{7}$$

Then we replace the boundary condition (7) with

$$\nu_e \frac{du_x^{BL}}{dy}|_{y=0} = R, \quad a_e \frac{d\theta^{BL}}{dy}|_{y=0} = S \tag{8}$$

Now we solve the initial value problem (6), (8) using a shooting method for (R, S) until conditions (7) are fulfilled. Then we find the r.h.s. $\tau_t = U_*^2 \mathbf{u}/\|\mathbf{u}\|$ and $\dot{q}_0$ of the unknown wall boundary conditions for the outer solution by setting $U_*^2 = R$ and $\dot{q}_0 = c_p S$.

In the special case of a vanishing buoyancy force $\beta\theta^{BL} g_x$ in Ω_δ on the r.h.s. of the first equation of (6), we can avoid the shooting technique. We recover the standard wall functions (modified according to Reference [3]) in the *viscous sublayer* and in the *log-layer* as analytical solutions of (6), (7) using standard scaled variables

$$y^+ = yU_*/\nu, \quad u^+ = u_x^{BL}/U_*, \quad \theta^+ = c_p U_*(\theta_0 - \theta^{BL})/\dot{q}_0$$

The described DDM is realized as an iterative method within the discretization, decoupling, and linearization of the full model. A computational algorithm has to control that Γ_δ, being discretized with mesh points with minimal distance to Γ_0, belongs to the log-layer, see also Figure 2.

The mathematical foundation of the approach is open. Some ideas on how to proceed for the much simpler advection–diffusion problem are given in Reference [4].

3. DISCRETIZATION, DECOUPLING AND LINEARIZATION

We are mainly interested in the long-term integration of the model (1), (2) and apply the backward Euler scheme for the *semidiscretization in time*. On a partition $\{t_m\}_{m=0}^{M}$ of $[0,T]$ with $t_0=0,\ t_M=T$, we use the abbreviation $F^m=F(t_m)\equiv F(t_m,\cdot)$ for a function F. The time derivative is approximated as

$$\partial_t F(t_m)\approx \partial_t^m F=(F^m-F^{m-1})/\Delta_m$$

with time step $\Delta_m=t_m-t_{m-1}$. We arrive at the semidiscrete system

$$\begin{aligned}
\partial_t^m\mathbf{u}-\nabla\cdot(2\nu_e^m S(\mathbf{u}^m))+(\mathbf{u}^m\cdot\nabla)\mathbf{u}^m+\nabla p^m&=-\beta\theta^m\mathbf{g}\\
\nabla\cdot\mathbf{u}^m&=0\\
\partial_t^m\theta+(\mathbf{u}^m\cdot\nabla)\theta^m-\nabla\cdot(a_e^m\nabla\theta^m)&=(\dot q)^{V\,m}/c_p\\
\partial_t^m k+(\mathbf{u}^m\cdot\nabla)k^m-\nabla\cdot(\nu_k^m\nabla k^m)&=P_k^m+G^m-\varepsilon^m\\
\partial_t^m\varepsilon+(\mathbf{u}^m\cdot\nabla)\varepsilon^m-\nabla\cdot(\nu_\varepsilon^m\nabla\varepsilon^m)+C_2\frac{(\varepsilon^m)^2}{k^m}&=C_1\frac{\varepsilon^m}{k^m}(P_k^m+G^m)
\end{aligned}\tag{9}$$

Now we apply a block Gauss–Seidel method for the iterative decoupling and linearization of the system (9). A second upper index denotes the iteration step. Furthermore, we replace $\partial_t^m F$ by $\tilde\partial_t^m F:=(F^{m,i}-F^{m-1})/\Delta_m$. Given $\mathbf{u}^{m,0}$, $p^{m,0}$, $\theta^{m,0}$, $k^{m,0}$, $\varepsilon^{m,0}$ as the solutions of the previous time step, the linearization cycle (in each time step) reads:

(A) Initialization: Set $it_{dlc}\leftarrow 1$.
(B) Set $i\leftarrow it_{dlc}$ and update turbulent viscosity $\nu_t^m\leftarrow\nu_t^m(k^{m,i-1},\varepsilon^{m,i-1})$. Update $U_*,\dot q_0$ according to Section 2 using $\mathbf{u}^{m,i-1}$ and $\theta^{m,i-1}$.
(C) Update ν_e^m and solve the linearized Navier–Stokes equations

$$\begin{aligned}
\tilde\partial_t^m\mathbf{u}+(\mathbf{u}^{m,i-1}\cdot\nabla)\mathbf{u}^{m,i}-\nabla\cdot(2\nu_e^m S(\mathbf{u}^{m,i}))+\nabla p^{m,i}&=-\beta\theta^{m,i-1}\mathbf{g}\\
\nabla\cdot\mathbf{u}^{m,i}&=0
\end{aligned}$$

(D) Update a_e^m and solve the θ-equation

$$\tilde\partial_t^m\theta+(\mathbf{u}^{m,i}\cdot\nabla)\theta^{m,i}-\nabla\cdot(a_e^m\nabla\theta^{m,i})=(\dot q^V)^m/c_p$$

(E) Update ν_k^m, P_k^m, G^m using $\mathbf{u}^{m,i}$, $\theta^{m,i}$ and solve the k-equation

$$\tilde\partial_t^m k+(\mathbf{u}^{m,i}\cdot\nabla)k^{m,i}-\nabla\cdot(\nu_k^m\nabla k^{m,i})=P_k^m+G^m-\varepsilon^{m,i-1}$$

(F) Update P_k^m, G^m, ν_ε^m using $\mathbf{u}^{m,i}$, $\theta^{m,i}$, $k^{m,i}$ and solve the ε-equation

$$\tilde\partial_t^m\varepsilon+(\mathbf{u}^{m,i}\cdot\nabla)\varepsilon^{m,i}-\nabla\cdot(\nu_\varepsilon^m\nabla\varepsilon^{m,i})+C_2\frac{\varepsilon^{m,i-1}}{k^{m,i}}\varepsilon^{m,i}=C_1\frac{\varepsilon^{m,i-1}}{k^{m,i}}(P_k^m+G^m)$$

(G) Stopping criterion for linearization cycle: if $it_{dlc} < \max_{dlc}$ and if stopping criteria for $\{\mathbf{u}_i^{m,i}\}_i$, $\{\theta_i^{m,i}\}_i$, $\{k_i^{m,i}\}_i$, $\{\varepsilon_i^{m,i}\}_i$ are not yet fulfilled, then set $it_{dlc} \leftarrow it_{dlc} + 1$ and goto (B). Otherwise goto next time step.

The iterative scheme (A)–(G) requires the solution of two basic problems. First, the linearized equations for θ, k and ε are ADR problems with non-constant viscosity of the general form:

$$\begin{aligned} Lu \equiv -\boldsymbol{\nabla}\cdot(v\boldsymbol{\nabla}u) + (\mathbf{b}\cdot\boldsymbol{\nabla})u + cu = f \quad &\text{in } \tilde{\Omega} \\ u = g \quad &\text{on } \tilde{\Gamma}_D \\ v\boldsymbol{\nabla}u\cdot\mathbf{n} = h \quad &\text{on } \tilde{\Gamma}_N \end{aligned} \tag{10}$$

For θ we set $\tilde{\Omega}=\Omega$, $\tilde{\Gamma}_D=\Gamma_-$, $\tilde{\Gamma}_N=\Gamma_0\cup\Gamma_+$, $h|_{\Gamma_0}=\dot{q}_0/c_p$, $h|_{\Gamma_+}=0$. For k and ε set $\tilde{\Omega}=\Omega\backslash\Omega_\delta$, $\tilde{\Gamma}_D=(\Gamma_-\cap\partial\tilde{\Omega})\cup\Gamma_\delta$ with appropriate g and $\tilde{\Gamma}_N=\Gamma_+$ with $h=0$. The other data from (D)–(F) are given in the following table:

Equation	u	v	$\mathbf{b}$	cu	f
For θ	$\theta^{m,i}$	a_e^m	$\mathbf{u}^{m,i}$	$\theta^{m,i}/\Delta_m$	$\dot{q}^V/c_p + \theta^{m-1}/\Delta_m$
For k	$k^{m,i}$	ν_k^m	$\mathbf{u}^{m,i}$	$k^{m,i}/\Delta_m$	$(P_k^m + G^m) - \varepsilon^{m,i-1} + k^{m-1}/\Delta_m$
For ε	$\varepsilon^{m,i}$	ν_ε^m	$\mathbf{u}^{m,i}$	$C_2(\varepsilon^{m,i-1}/k^{m,i})\varepsilon^{m,i} + \varepsilon^{m,i}/\Delta_m$	$C_1(\varepsilon^{m,i-1}/k^{m,i})(P_k^m + G^m) + \varepsilon^{m-1}/\Delta_m$

Later on, we simply write Ω and omit the indices of viscosities and production terms.

The linearized Navier–Stokes equations are of *Oseen*-type with a positive reaction term and non-constant viscosity

$$\begin{aligned} L_O(\mathbf{a},\mathbf{u},p) \equiv -\boldsymbol{\nabla}\cdot(2\nu S(\mathbf{u})) + (\mathbf{a}\cdot\boldsymbol{\nabla})\mathbf{u} + c\mathbf{u} + \boldsymbol{\nabla}p = \mathbf{f} \quad &\text{in } \Omega \\ \boldsymbol{\nabla}\cdot\mathbf{u} = 0 \quad &\text{in } \Omega \\ (\tau - pI)\mathbf{n} = \tau_n\mathbf{n} \quad &\text{on } \Gamma_-\cup\Gamma_+ \\ (I - \mathbf{n}\otimes\mathbf{n})2\nu_e S(\mathbf{u})\mathbf{n} = \boldsymbol{\tau}_t, \quad \mathbf{u}\cdot\mathbf{n} = 0 \quad &\text{on } \Gamma_0 \end{aligned} \tag{11}$$

Comparison with step (C) of the linearization cycle yields $\mathbf{u}=\mathbf{u}^{m,i}$, $\nu=\nu_e$, $\mathbf{a}=\mathbf{u}^{m,i-1}$, $c=1/\Delta_m$, $p=p^{m,i}$, $\mathbf{f}=-\beta\theta^{m,i-1}\mathbf{g}+c\mathbf{u}^{m-1}$.

For the finite element discretization of (10)–(11) we assume an admissible triangulation $\mathcal{T}_h=\{K\}$ of the Lipschitz domain Ω and define finite element subspaces $X_h^l \equiv \{v\in C(\bar{\Omega}) \mid v|_K \in \Pi_l(K)\ \forall K\in\mathcal{T}_h\}$, $l\in\mathbf{N}$. Furthermore, $(\cdot,\cdot)_S$ denotes the inner product on some S.

For the ADR problem (10), for simplicity with $g=0$ on Γ_D, we apply the Galerkin-FEM with SUPG-stabilization:

$$\begin{aligned} &\text{find } u\in V_h=\{v\in X_h^l \mid v|_{\Gamma_D}=0\} \quad \text{s.t.: } b^s(u,v)=l^s(v) \quad \forall v\in V_h \\ &b^s(u,v)=(v\nabla u,\nabla v)_\Omega+((\mathbf{b}\cdot\nabla)u+cu,v)_\Omega+\sum_{T\in\mathscr{T}_h}(\delta_T Lu,(\mathbf{b}\cdot\nabla)v)_T \\ &l^s(v)=(f,v)_\Omega+(h,v)_{\Gamma_N}+\sum_{T\in\mathscr{T}_h}(\delta_T f,(\mathbf{b}\cdot\nabla)v))_T \end{aligned} \tag{12}$$

with appropriate parameter set $\{\delta_T\}_T$, see Reference [5]. The SUPG solutions may suffer from local crosswind oscillations in layers; this is, in particular, the case for the temperature field θ. Furthermore, (unphysical) negative values of k or ε can occur. As a remedy, we add in a consistent way crosswind diffusion thus leading to the (non-linear) shock-capturing method, for details see Reference [1].

For the Oseen-problem (11), we define the discrete spaces $\mathbf{V}_h\times Q_h=(X_h^r)^d\times X_h^s$ with $r,s\in\mathbf{N}$. The Galerkin-FEM requires the (bi)linear forms

$$\mathscr{A}(U,V)=a(\mathbf{u},\mathbf{v})+b(\mathbf{v},p)-b(\mathbf{u},q), \quad \mathscr{L}(V)=L(\mathbf{v})$$

with $U=(\mathbf{u},p)$, $V=(\mathbf{v},q)$ and $b(\mathbf{v},p)=-\int_\Omega p(\nabla\cdot\mathbf{v})\,\mathrm{d}x$. Furthermore, set

$$\begin{aligned} a(\mathbf{u},\mathbf{v})&=(2\nu S(\mathbf{u}),\nabla\mathbf{v})_\Omega+((\mathbf{a}\cdot\nabla)\mathbf{u}+c\mathbf{u},\mathbf{v})_\Omega+((pI-\mathbf{n}\otimes\mathbf{n}\tau)\mathbf{n},\mathbf{v})_{\Gamma_0} \\ L(\mathbf{v})&=(\mathbf{f},\mathbf{v})_\Omega+(\tau_n\mathbf{n},\mathbf{v})_{\Gamma_-\cup\Gamma_+}+(\boldsymbol{\tau}_t,\mathbf{v})_{\Gamma_0} \end{aligned}$$

When using equal order ansatz functions $r=s$, the discrete Babuska–Brezzi condition is not satisfied. This problem is circumvented using a pressure (PSPG) stabilization. In addition, divergence and SUPG-stabilizations are used to deal with dominating first-order terms. More precisely, we set

$$\begin{aligned} \mathscr{A}^s(U,V)&=\mathscr{A}(U,V)+\sum_{T\in\mathscr{T}_h}[(L_O(\mathbf{a},\mathbf{u},p),\delta_{1u}^T(\mathbf{a}\cdot\nabla)\mathbf{v}+\delta_{1p}^T\nabla q)_T+\delta_{2u}^T(\nabla\cdot\mathbf{u}),(\nabla\cdot\mathbf{v})_T] \\ \mathscr{L}^s(V)&=\mathscr{L}(V)+\sum_{T\in\mathscr{T}_h}(\mathbf{f},\delta_{1u}^T(\mathbf{a}\cdot\nabla)\mathbf{v}+\delta_{1p}^T\nabla q)_T \end{aligned}$$

Finally, the stabilized problem to the Oseen equation (11) reads:

$$\text{find } U=(\mathbf{u},p)\in\mathbf{V}_h\times Q_h \quad \text{s.t. } \mathscr{A}^s(U,V)=\mathscr{L}^s(V) \quad \forall V\in\mathbf{V}_h\times Q_h \tag{13}$$

For the choice of the stabilization parameters δ_{1u}^T, δ_{2u}^T, and δ_{1p}^T see Reference [5].

4. DOMAIN DECOMPOSITION OF THE LINEARIZED PROBLEMS

A non-overlapping domain decomposition method with Robin interface conditions is applied to the basic linearized problems (10), (11). Consider a non-overlapping partition of Ω into convex, polyhedral subdomains being aligned with the finite element mesh (FEM), i.e.

$$\bar\Omega=\bigcup_{k=1}^N\bar\Omega_k, \quad \Omega_k\cap\Omega_j=\emptyset \quad \forall k\neq j, \quad \forall K\in\mathscr{T}_h\ \exists k\colon K\subset\Omega_k$$

Furthermore, set $\Gamma_k := \partial\Omega_k \backslash \partial\Omega$, $\Gamma_{jk} := \partial\Omega_j \cap \partial\Omega_k$, $j \neq k$, where Γ_{kj} is identified with Γ_{jk}. Assume, for simplicity, that the partition is stripwise.

For the (continuous) ADR problem (10) the DDM reads: for given u_k^n from iteration step n on each Ω_k, seek (in parallel) for u_k^{n+1}

$$\begin{aligned} Lu_k^{n+1} &= f \quad \text{in } \Omega_k \\ u_k^{n+1} &= 0 \quad \text{on } \Gamma_D \cap \partial\Omega_k \\ \nu \nabla u_k^{n+1} \cdot \mathbf{n}_k &= h \quad \text{on } \Gamma_N \cap \partial\Omega_k \end{aligned}$$

together with the *interface conditions*

$$\Phi_k(u_k^{n+1}) = \theta \Phi_k(u_j^n) + (1-\theta)\Phi_k(u_k^n) \quad \text{on } \Gamma_{jk}, \ j = 1, \ldots, N, \ j \neq k$$

with a relaxation parameter $\theta \in (0, 1]$. The interface function is specified as

$$\Phi_k(u) = \nu \nabla u \cdot \mathbf{n}_k + (-\tfrac{1}{2}\mathbf{b} \cdot \mathbf{n}_k + z_k)u \tag{14}$$

Let $V_{k,h}$, b_k^s and l_k^s denote the restrictions of V_h, b^s and l^s to Ω_k, respectively. $W_{kj,h}$ is the restriction of V_h to the interface part Γ_{kj}. Furthermore, $\langle \cdot, \cdot \rangle_{\Gamma_{kj}}$ is the inner product in $L^2(\Gamma_{kj})$ or, whenever needed, the dual product in $(W_{kj,h})^* \times W_{kj,h}$. The *fully discretized* DDM reads for $k = 1, \ldots, N$:

Parallel computation step: find $u_k^{n+1} \in V_{k,h}$ such that $\forall v_k \in V_{k,h}$

$$b_k^s(u_k^{n+1}, v_k) + \langle (-\tfrac{1}{2}\mathbf{b} \cdot \mathbf{n}_k + z_k) u_k^{n+1}, v_k \rangle_{\Gamma_k} = l_k^s(v_k) + \sum_{j(\neq k)} \langle \Lambda_{jk}^n, v_k \rangle_{\Gamma_{kj}}$$

Communication step: for all $j \neq k$, update the Lagrangian multipliers

$$\langle \Lambda_{kj}^{n+1}, \phi \rangle_{\Gamma_{kj}} = \langle \theta(z_k + z_j) u_k^{n+1} - \theta \Lambda_{jk}^n + (1-\theta)\Lambda_{kj}^n, \phi \rangle_{\Gamma_{kj}} \quad \forall \phi \in W_{kj,h}$$

The analysis of the method, given in Reference [6], can be easily extended to the case of non-constant viscosity ν: The algorithm is well-posed if $z_k = z_j > 0$. The sequences $\{u_k^n\}_n$, $k = 1, \ldots, N$ converge strongly to the restrictions of the global discrete solution to Ω_k w.r.t. the stabilized energy norm induced by the symmetric part of $b_k^s(\cdot, \cdot)$.

An *a posteriori estimate* (given in Reference [6] for two subdomains) allows to control the convergence on subdomains via jumps of discrete DD solutions across the interface. Besides this estimate allows the following design of the interface function:

$$\begin{aligned} z_k &= \tfrac{1}{2}|\mathbf{b} \cdot \mathbf{n}_k| + R_k \\ R_k &\sim \frac{\nu_{\min}}{H} \left[1 + H \sqrt{\frac{c_{\max}}{\nu_{\min}}} + \min \left(\frac{\|\mathbf{b}\|_{\max}}{\sqrt{(\nu c)_{\min}}}; \frac{H \|\mathbf{b}\|_{\max}}{\nu_{\min}} \right) \right] \end{aligned} \tag{15}$$

where H is the diameter of the interface. Equation (15) is compatible with the vanishing viscosity limit $\nu \to 0$. Moreover, it is shown in Reference [6] that (15) is surprisingly sharp w.r.t. data and allows a considerable acceleration of convergence.

For the Oseen problem (11) we use the abbreviation $\pi_{t,k} := I - \mathbf{n}_k \otimes \mathbf{n}_k$. Then the DDM is defined as follows: for given $(\mathbf{u}_k^n, p_k^n)$ from step n on each Ω_k, seek (in parallel)

for $(\mathbf{u}_k^{n+1}, p_k^{n+1})$

$$
\begin{aligned}
L_{\mathrm{O}}(\mathbf{a}, \mathbf{u}_k^{n+1}, p_k^{n+1}) &= \mathbf{f} \quad \text{in } \Omega_k \\
\boldsymbol{\nabla} \cdot \mathbf{u}_k^{n+1} &= 0 \quad \text{in } \Omega_k \\
(\tau_k^{n+1} - p_k^{n+1} I)\mathbf{n}_k &= \tau_n \mathbf{n}_k \quad \text{on } \partial\Omega_k \cap (\Gamma_- \cup \Gamma_+) \\
\pi_{t,k} \tau_k^{n+1} \mathbf{n}_k = \boldsymbol{\tau}_{\mathrm{t}}, \quad -\mathbf{u}_k^{n+1} \cdot \mathbf{n}_k &= 0 \quad \text{on } \partial\Omega_k \cap \Gamma_0
\end{aligned}
$$

together with the interface conditions

$$
\Phi_k(\mathbf{u}_k^{n+1}, p_k^{n+1}) = \theta \Phi_k(\mathbf{u}_j^n, p_j^n) + (1-\theta)\Phi_k(\mathbf{u}_k^n, p_k^n) \quad \text{on } \Gamma_{jk}
$$

$\theta \in (0, 1]$ is again a relaxation parameter. The interface function is given by

$$
\Phi_k(u, p) = \nu \boldsymbol{\nabla} \mathbf{u} \cdot \mathbf{n}_k - p\mathbf{n}_k + (-\tfrac{1}{2}\mathbf{a} \cdot \mathbf{n}_k + z_k)\mathbf{u} \tag{16}
$$

with acceleration parameter z_k.

The corresponding parallel algorithm can be formulated (in weak form) similarly as for the scalar case. For this DD algorithm (and certain variants of it), a similar *a priori* and *a posteriori* analysis is available as briefly described for the scalar problem (10). In particular, the interface function z_k in (16) has the same structure as in (15). For details, we refer to References [7, 8].

5. APPLICATION TO ROOM-AIR FLOW SIMULATION

We implemented the stabilized FEM of Section 3 within our research code *Parallel NS*. Piecewise linear ansatz functions are used for all unknowns ($l = r = s = 1$) on unstructured tetrahedral (resp. triangular) meshes in 3D (resp. 2D). The DDM of Section 4 is parallelized using a master/slave paradigm in the PVM configuration; it has been implemented on a cluster of Linux workstations connected by Ethernet. No coarse-grid solver is used so far; hence, the application is restricted to the coarse-granular case.

The validation of the approach to *laminar* flows has been considered e.g. in References [7, 8]. For the *turbulent* case, cf. Sections 1 and 2, the validation of the approach for typical test cases (e.g. the standard 2D Cheesewright test in a closed cavity or a 3D flow in a cavity with large opening) is given in Reference [9, Chapter 4], Here we present two examples.

Example 1

Natural convection 3D closed cavity. This is a benchmark problem with Rayleigh number $Ra = 2.3 \times 10^{10}$ in the cubic box Ω. The problem data, the surface mesh, and the induced vector and temperature fields are shown in Figure 3. Here we want to demonstrate the influence of the overlapping DDM together with the boundary layer iteration, cf. Section 2. Alternatively, a resolution of the wall layer region would require a maximal aspect ratio of $\mathcal{O}(\sqrt{Ra})$ for the elements nearest to the wall. The quasi-stationary solution can be computed with relatively large time steps.

The turbulent heat flows (in Watt) $\dot{Q}_{\mathrm{in}}/W$ resp. $\dot{Q}_{\mathrm{out}}/W$ on the 'cooled' wall at $y = 0$ and on the 'heated' wall at $y = 1$, respectively, are shown in Table I in dependence of the layer

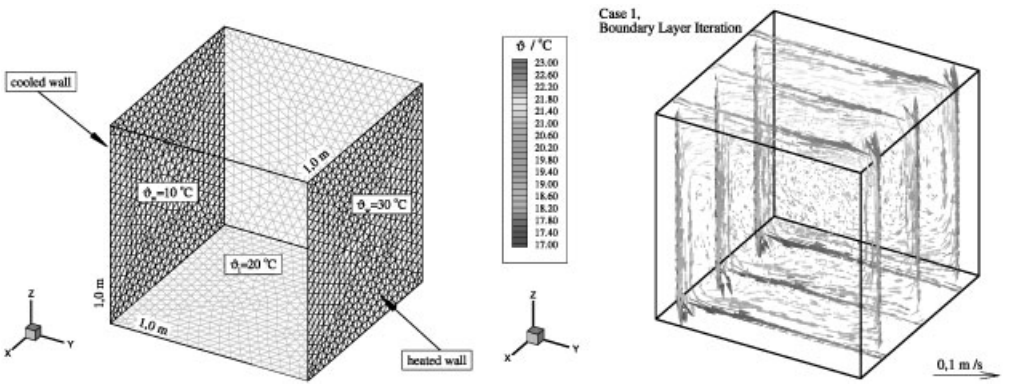

Figure 3. Natural convection in a 3D closed cavity.

Table I. Turbulent heat flow in dependence of layer width δ.

Width δ (m)	0.005	0.02	0.04	0.06	0.08	0.1	
# of elements	35.924	29.535	19.382	15.778	12.436	6.485	
Wall	−41.6	−12.5	−6.32	−3.81	−3.29	−2.10	$\dot{Q}_{\text{out}}/W$
function	40.9	12.3	6.17	3.72	3.10	1.96	$\dot{Q}_{\text{in}}/W$
Layer	−46.5	−32.1	−36.0	−33.9	−32.2	−25.2	$\dot{Q}_{\text{out}}/W$
iteration	46.3	31.5	35.3	33.4	31.8	24.7	$\dot{Q}_{\text{in}}/W$

width δ. The application of the boundary layer iteration is remarkably more robust than the application of standard wall functions.

The turbulent heat flow data in the 'sequential' case agree very well with those of a parallel computation using a coarse-granular $2 \times 2 \times 2$ partition of Ω.

Example 2

Air flow simulation in an office with opened window. In Figure 4 we show an unfurnished office and its coarse-granular decomposition into 4 subdomains. Furthermore, different variants of an opened window and details of the surface FEM are shown. Details of the simulation with roughly 150.000 tetrahedral elements over a period of 3.600 s with time step of 1 (s) are given in Reference [9]. Here we want to point out some interesting observations: First, the inflow and outflow zones Γ_- and Γ_+ are well described by the boundary conditions (3), (5), see also Figure 5. Let us mention that the solution is not disturbed by the interaction of the window with the subdomain partition. Secondly, in comparison with the sequential solution, we obtained a speed up of 3.76 on a cluster of 4 AMD Athlon 1 GHz processors.

As a final example we consider the air flow simulation in the same office with furnishing and an partly opened window. In Figure 5 we show a snap-shot of the calculated flow field for two variants where the monitor is switched off and on, respectively. Details of the

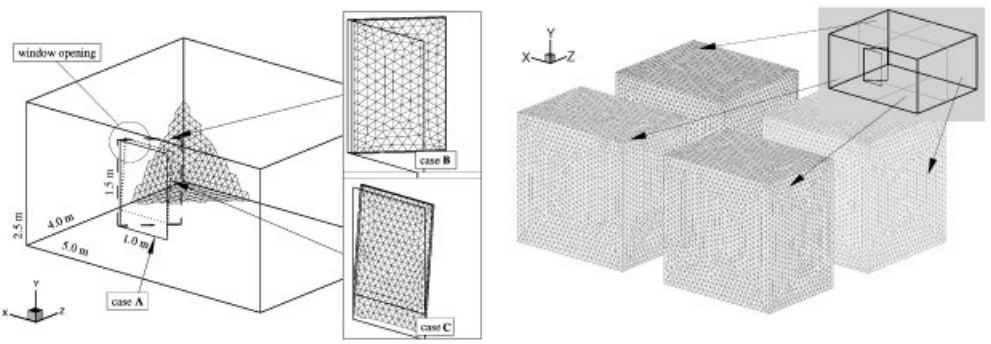

Figure 4. Geometrical model and coarse-granular decomposition of an office.

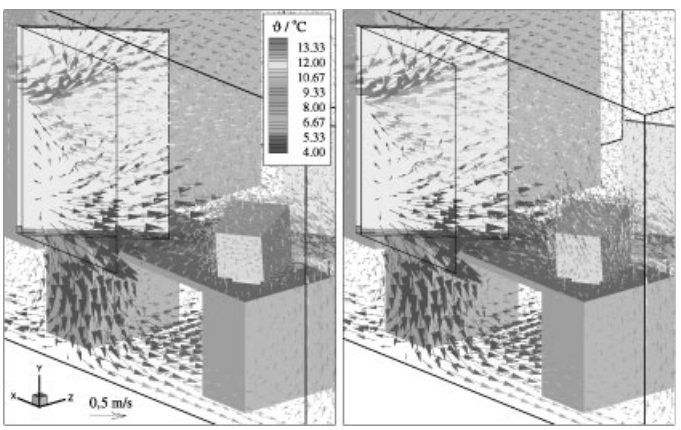

Figure 5. Two variants of the flow field in an office—enlarged view.

calculations and on the prediction of certain parameters of the indoor air climate can be found again in Reference [9]. The comparison of the numerical results with experimental data is in preparation.

These and other numerical results indicate that the approach is suitable for the parallel numerical simulation of indoor air flows in the coarse–granular case. The method is now applied at the Dresden University of Technology to the simulation of turbulent indoor air flows. Such calculations allow to predict certain parameters of the indoor air climate over longer periods and to simulate different variants of ventilation or of heating systems. Future research will be concerned with other turbulence models, improved iterative substructuring method based on Dirichlet-Robin coupling, see Reference [1], and with coarse-grid solvers.

REFERENCES

1. Codina R, Soto O. Finite element implementations of two-equation and algebraic stress turbulence models for steady incompressible flow. *International Journal for Numerical Methods in Fluids* 1999; **90**(3):309–334.
2. Mohammadi B, Pironneau O. *Analysis of the K-Epsilon Turbulence Model*. Wiley: New York, 1994.
3. Neitzke KP. The behaviour of the flow in rooms. Near walls measurements and computations. *Proceedings of the 6th International Conference on Air Distributions in Rooms*, vol. 2. Stockholm, Sweden, 1998; 293–298.
4. Le Tallec P, Tidiri MD. Convergence analysis of domain decomposition algorithms with full overlapping for the advection–diffusion problems. *Mathematics of Computation* 1999; **68**:585–606.
5. Roos HG, Stynes M, Tobiska L. *Numerical Methods for Singularly Perturbed Differential Equations*. Springer: Berlin, 1996.
6. Lube G, Müller L, Otto FC. A non-overlapping domain decomposition method for the advection–diffusion problem. *Computing* 2000; **64**:49–68.
7. Lube G, Müller L, Otto FC. A non-overlapping domain decomposition method for stabilized finite element approximations of the Oseen equations. *Journal of Computational and Applied Mathematics* 2001; **132**: 211–236.
8. Lube G, Müller L, Müller H. A new non-overlapping domain decomposition method for stabilized finite element methods applied to the non-stationary Navier–Stokes equations. *Numerical Linear Algebra with Applications* 2000; **7**:449–472.
9. Gritzki R. Numerical simulation of the efficiency of user-defined window ventilation. *Ph.D. Thesis*, TU Dresden, 2001 (in German).
10. Achdou Y, Le Tallec P, Nataf F, Vidrascu M. A domain decomposition preconditioner for an advection–diffusion problem. *Computer Methods in Applied Mechanics and Engineering* 2000; **184**:145–170.

